Polymer 351 (2026) 129825

Contents lists available at ScienceDirect

Polymer

journal homepage: www.elsevier.com/locate/polymer

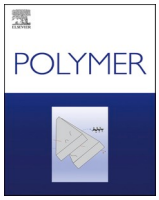

On the production and application of functional branched oligomers by PLA upcycling using a green solvent-based approach

Martina Cozzani [a], Alessandro Fortunato [a], Giacomo Damonte [a], Alessandro Pellis [a], Donatella Di Lisa [b,c], Laura Pastorino [b,c], Orietta Monticelli [a,*]

[a] Dipartimento di Chimica e Chimica Industriale, Università di Genova, Via Dodecaneso 31, 16146, Genova, Italy
[b] Dipartimento di Informatica, Bioingegneria, Robotica e Ingegneria dei Sistemi, Università di Genova, Via All'Opera Pia 13, 16145, Genova, Italy
[c] IRCCS Ospedale Policlinico San Martino, Largo Rosanna Benzi 10, 16132, Genova, Italy

A B S T R A C T

The main goal of this work was to develop an environmentally friendly method for upcycling poly (lactic acid) (PLA) into functionalized oligomers, as well as to propose an innovative strategy enabling their direct use within the reaction environment. To this end, the investigated reaction—an alcoholysis based on the use of reagents derived from renewable sources—was carried out in the green solvent dihydrolevoglucosenone (Cyrene®, Cy). Indeed, upon the addition of virgin polymer, a PLA/oligomer mixture was obtained, providing a suitable system for the direct preparation of porous films. Specifically, the alcoholysis process, carried out using pentaerythritol (PE) as the polyalcohol and zinc stearate as the catalyst was optimized by monitoring the viscosity of the reaction mixture over time. ^{1}H NMR analysis of the resulting oligomers confirmed a decrease in molecular weight and the formation of a branched structure, attributed to the multifunctionality of the polyalcohol and dependent on the amount of PE added. These structural characteristics significantly affected the thermal behaviour of the oligomers, as demonstrated by DSC and TGA analyses.

Porous films, prepared via the Non-solvent Induced Phase Separation (NIPS) technique using the reaction mixture directly as the casting solution, exhibited a leaf-like structure that was unaffected by the presence of oligomers in the mixture, as observed by FE-SEM analysis.

The enzymatic hydrolysability and retention capacity were evaluated using *Humicola insolens* cutinase (HiC) as the enzyme and pararosaniline hydrochloride (PARA) as a cationic organic dye, selected to mimic the behavior of amino-terminated drugs. The results indicated that, compared to neat PLA films, those incorporating the developed oligomers exhibited enhanced dye retention capacity and faster degradation rate. These phenomena were attributed to the high functionality of the branched additives obtained through the alcoholysis process. Finally, a closed-loop process for Cy recovery through distillation was established, enabling its reuse and improving the overall sustainability of the process.

1. Introduction

The recycling of polymer materials is of great importance for our economy [1,2], the development of which must consider both the applicability of the resulting compounds and the use of environmentally friendly methods. These requisites apply to bioplastics, as it is necessary to use conditions that meet the requirements of the circular economy, which characterizes the production and end of life of this type of material [3–5].

In the case of PLA, the subject of the study, recycling can be carried out using both physical and chemical methods. Mechanical recycling is generally characterized by simplicity, cost-effectiveness and easy scalability [6], but can be associated with collateral degradation processes due to mechanical stresses and high temperatures [7], making the use of antioxidant agents or chain extenders necessary [8,9]. In particular, a decrease in molecular weight due to chain scissions after mechanical recycling processes was generally observed [10]. As underlined by Badia et al., [11] this leads to a significant deterioration in material performances after only two reprocessing steps. Żenkiewicz et al. demonstrated that multiple recycling cycles resulted in a decrease in the mechanical properties of PLA as well as a significant increase in melt flow rate [12]. Brüster et al. also reported comparable behaviour in plasticized PLA, which was no longer suitable for recycling or reuse for its intended application after reprocessing processes [13]. On the other hand, chemical recycling approaches lead to the fragmentation of polymer chains and conversion of the polymers into low molecular weight products with significant added value [14], which can be used for direct re-polymerization or other applications [15,16]. However, chemical recycling is generally based on the application of impactful separation and purification steps, which makes it difficult to scale-up the entire process. As far as the application of this process to PLA is concerned, alcoholysis has proven to be a particularly promising method, as

* Corresponding author.
E-mail address: orietta.monticelli@unige.it (O. Monticelli).

https://doi.org/10.1016/j.polymer.2026.129825
Received 7 January 2026; Received in revised form 20 February 2026; Accepted 6 March 2026
Available online 6 March 2026

it has relatively low requirements in terms of conditions compared to other recycling techniques, even if it is subjected to the above-mentioned limitations [17]. In this scenario, an innovation over traditional alcoholysis approach was proposed by Damonte et al., [18] who demonstrated the possibility of applying this approach under molten conditions without requiring any purification steps of the resulting products. Indeed, the branched compounds obtained were successfully used in a formulation with a bio-based multifunctional epoxide.

In this work, the recycling of PLA was extended to a chemical process based on the application of an alcoholysis reaction in a solvent capable of dissolving both the polymer and the polyalcohol. Although this approach appears to be less effective than the melt blending process, as it relies on the use of a solvent, it was developed to adapt the upcycling of the alcoholysis products to a specific application, considering both sustainability and scalability. Indeed, the method developed consists of a closed loop based on the use of i) a solvent from renewable sources, namely dihydrolevoglucosenone (Cyrene®, Cy), in which the alcoholysis reaction takes place, ii) the same system without the need for purification or treatment after the addition of a virgin PLA to produce porous films and iii) the recovery of the solvent used in the depolymerization reaction. In this context, it is important to underline that porous films based on PLA are systems of considerable application interest. Indeed, they combine the properties of the polymer matrix, such as the origin from renewable sources, biodegradability and biocompatibility, with the features given by the particular geometry, especially in terms of porosity and mechanical properties.

The interest in these materials is evidenced by some recent works highlighting different preparation methods - e.g. phase separation, electrospinning, 3D printing - and various potential applications of the films, such as the biomedical sector and the field of separation [19–27]. In this context, an important aspect for the application of the films needs to be addressed: their functionalization, a property that the polymer matrix does not possess. In the case of PLA, the functionalization affecting the surface was achieved by applying various chemical or physical methods [28–32], or by adding inorganic and organic additives when the bulk was also involved [33,34]. In the latter approach, to improve the dispersibility of the additive, its compatibility with the polymer matrix must be taken into account, a property that can be improved by suitably designing its chemical structure. In this regard, additives that have a branched geometry and are therefore characterized by high functionality but hold arms with the same chemical structure as PLA, are the most suitable.

On this basis, and taking into account the possibility of upcycling products from the alcoholysis of PLA, a process was developed in a solvent in which not only a depolymerization reaction could take place, leading to the formation of branched oligomers, but which is also suitable for the preparation of mixtures for the development of porous films, *i.e.*, in which both the virgin polymer and the additives can be dissolved. Therefore, unlike other functionalization methods, such as blending with other polymers or additives, which require the preliminary preparation and purification of these compounds, our approach is based on matrix-compatible, highly functionalized additives and on an alternative incorporation strategy that does not involve expensive or environmentally impactful steps and is therefore easily scalable.

In particular, the alcoholysis reaction was studied starting from a commercially available high molecular weight PLA in Cy using pentaerythritol (PE) as polyalcohol and Zn stearate as catalyst, two compounds from renewable sources. In particular, regarding the choice of catalyst, it is important to underline that this compound, in addition to being active in the transesterification reaction of polyesters under molten conditions [35], possesses properties that make it suitable for use in polymeric materials as a plasticiser [36], as well as in cosmetics [37], due to its biocompatibility. In the developed formulation, since the catalyst is not removed, the above characteristic is essential for the production of films that can be used as drug carriers. The oligomers obtained by changing the amount of PE in the reaction mixture were characterized in detail by ^{1}H NMR, DSC and TGA measurements. A virgin PLA was added to the same reagent mixture without purification steps and, after solubilization of the components, porous films were prepared by applying the simple Non-solvent Induced Phase Separation (NIPS) technique using deionised water as a non-solvent system (Fig. 1). The films containing the different oligomeric systems from the alcoholysis reactions were analysed in terms of their thermal, morphological, adsorption, biocompatibility and degradation properties. Finally, the possibility of recovering Cy, used in the preparation of films and containing water and low molecular weight compounds, was evaluated.

2. Experimental section

2.1. Materials

Poly (lactic acid) (PLA) Luminy LX175 (M_n = 100000 g/mol, melt flow index (MFI) = 6.0 g/10 min) was purchased from Corbion. Dihydrolevoglucosenone (Cyrene®, Cy) (purity ≥98.0%), pentaerythritol (PE) (purity ≥99.0%), pararosaniline hydrochloride (PR) (purity ≥85%), and KPO buffer salts (KH_2PO_4 and K_2HPO_4) were purchased from Sigma-Aldrich and used as received. Technical grade Zinc stearate (Zn stearate) was purchased from Faci S.p.A (Italy). *Humicola insolens* Cutinase (HiC) (Novozym® 51032, product code: 06-3135) was purchased from STREM Chemicals.

2.2. Preparation of PLA oligomers via alcoholysis reactions

Post-consumer PLA with a high molecular weight was subjected to alcoholysis reactions using PE. For each reaction, 2.0 g of PLA pellets, previously dried in a vacuum oven, were used. PLA was placed in a two-neck round bottom flask equipped with a stainless-steel stirrer and solubilised in 10 mL of Cy, with the temperature maintained at 100 °C and in an inert atmosphere obtained by means of argon flow. Subsequently, the polyalcohol was added in varying concentrations, *i.e.* 2, 5 or 10 wt% with respect to the weight of the mixture consisting of PLA, polyalcohol and catalyst. Following the complete solubilization of the polyalcohol, the catalyst, namely Zn stearate, was added at a concentration of 2 wt% by weight of the mixture. The alcoholysis reaction was then sustained for a 72-h period, during which the system was maintained at a temperature of 100 °C and subjected to continuous stirring. Some samples were purified for ^{1}H NMR and thermal analysis by slowly dropping the solution into deionised water while stirring vigorously. The system was then filtered through a Büchner funnel and washed twice more with deionised water to remove Cy and unreacted PE. Finally, the product was dried under vacuum at room temperature for three days.

The alcoholysis products were named according to the concentration of pentaerythritol, e.g. the oligomer obtained using 10 wt% of pentaerythritol is denoted as PLA_PE10.

2.3. Porous films preparation

The polymer solutions used for the development of porous films were prepared by the direct addition of high-molecular-weight PLA into the alcoholysis reaction systems described above, maintaining a concentration of 20% w/v in Cy. The ratio of PLA to alcoholysis products was set at 80/20% w/w, with the type of oligomer (namely PLA_PE2, PLA_PE5, and PLA_PE10) serving as the only variable. The films were prepared via Non-solvent Induced Phase Separation (NIPS) technique. The polymer solutions were cast onto a glass substrate, using a doctor blade to obtain films with a thickness of 0.7 mm, allowing them to air-cool for approximately 30 s. Subsequently, the glass plate was immersed in a coagulation bath, filled with deionised water at 25 °C, for 24 h. The films were then subjected to three washes of 24 h each in deionised water. Thereafter, they were dried at room temperature for 72 h and

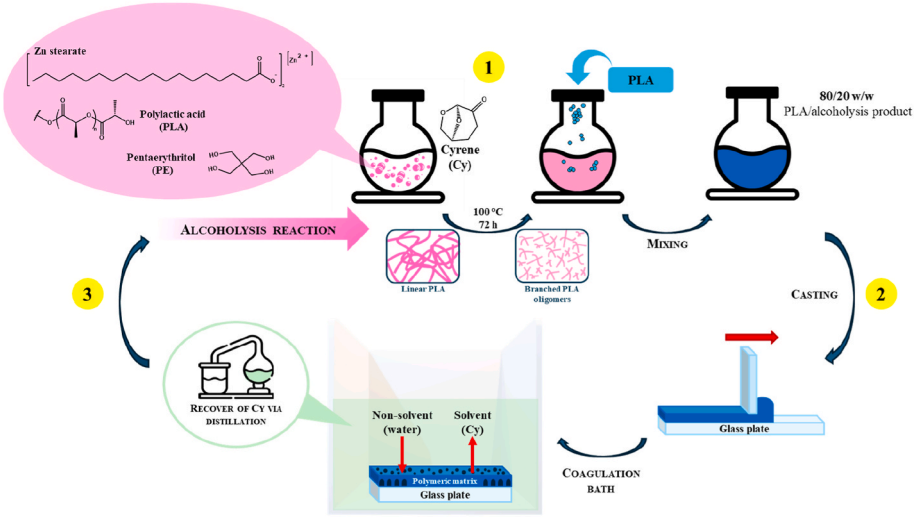

Fig. 1. Schematic representation of the work: (1) development of branched PLA oligomers through an alcoholysis process using PE as a polyol, zinc stearate as a catalyst, and Cy as a solvent, (2) preparation of porous films based on high-molecular-weight PLA and alcoholysis products via NIPS technique, (3) recovery of the solvent by distillation of the of water/Cy mixture derived from the film-development step.

placed in a vacuum oven at 30 °C for one week.

To facilitate clear identification of the films, they were named according to the alcoholysis product added to the PLA matrix, e.g. m_PLA_PE5 refers to the film with PLA_PE5 present in 20 wt% with respect to high-molecular-weight PLA.

2.4. Characterization

2.4.1. ^1H NMR analysis

Proton nuclear magnetic resonance (^{1}H NMR) analysis was conducted on alcoholysis products and on distillation residue of Cy.

The measurements were performed using a Bruker Avance 500 MHz spectrometer (Bruker, Karlsruhe, Germany) at 25 °C on 30 mg/mL solutions prepared in $CDCl_3$ containing 0.03% tetramethylsilane (TMS) as internal reference.

The mean molecular weight of the oligomers obtained via alcoholysis reactions was calculated by applying Equation (1).

$$M_n = DP \cdot \frac{M_{LA}}{2} = \left(\frac{A_{(a)}}{A_{(a')}} + 1\right) \cdot \frac{M_{LA}}{2} \quad (1)$$

Where DP is the degree of polymerization, $A_{(a)}$ corresponds to the area of the signal at 5.16 ppm, $A_{(a')}$ is the area of the signal at 4.35 ppm, and M_{LA} is the molecular weight of lactide, which is equal to 144.13 g/mol.

2.4.2. Thermal analysis

The thermal properties of PLA oligomers and porous films were investigated via DSC and TGA analysis. DSC was performed with a Mettler Toledo DSC1 STAR^e System® differential scanning calorimeter. The analysis was carried out between −10 and 200 °C, with a heating/cooling rate of ±10 °C/min and a nitrogen flow rate of 20 mL/min. TGA measurements were performed from 30 to 800 °C, with an heating rate of +20 °C/min and under a nitrogen flow of 80 mL/min, using the instrument Mettler Toledo TGA1 STAR^e System®.

2.4.3. Viscosity measurements

The viscosity of the alcoholysis reaction systems was analysed over time, with measurements taken after 24, 48 and 72 h of reaction. Additionally, analysis was performed on the polymer solutions utilised for the preparation of porous films. These tests were carried out using the Lamy RM200 CP4000 plus® cone-plate rheometer, equipped with a 60 mm spindle (CP60-20), and operating at 100 °C. The shear rate ranged from 10 to 100 s^{-1}, and the average of 10 viscosity values was measured.

2.4.4. Porosity measurement of porous films

The porosity of films was determined by applying Equation (2), which considers the density of the film (ρ_f) and the density of the polymer (ρ_p).

$$Porosity\ [\%] = \left(1 - \frac{\rho_f}{\rho_p}\right) \cdot 100 \quad (2)$$

Where ρ_f and ρ_p were calculated as shown in Equation (3) and Equation (4):

$$\rho_f = \frac{m_f}{V_f} \quad (3)$$

$$\rho_p = \frac{m_p}{V_p} = \frac{m_{p1} + m_{p2}}{V_{p1} + V_{p2}} = \frac{m_{p1} + m_{p2}}{\frac{m_{p1}}{\rho_{p1}} + \frac{m_{p2}}{\rho_{p2}}} = \frac{1}{\frac{X_{p1}}{\rho_{p1}} + \frac{X_{p2}}{\rho_{p2}}} \quad (4)$$

Where m_f is the mass of the film and V_f is its volume, while m_p and V_p denote the mass and the volume of the polymer, respectively. The volume of the polymer was calculated by considering the weight fractions of high-molecular-weight PLA and PLA oligomers present in each formulation (X_{p1} and X_{p2}, respectively) and their density (ρ_{p1} and ρ_{p2}, respectively), which was assumed to be identical for PLA and alcoholysis products, so equal to 1.26 g/cm^3.

2.4.5. Morphological analysis of porous films

The morphology of the porous films was analysed using a Zeiss Supra 40 VP Field Emission Scanning Electron Microscope (FE-SEM) equipped with a backscattered electron detector. Prior to imaging, the samples were cryogenically fractured by immersion in liquid nitrogen and subsequently coated with a thin graphite layer using a Polaron E5100.

2.5. Enzymatic hydrolysis experiments

Enzymatic hydrolysis tests were performed on rectangular specimens (approximately 0.5 × 1.0 cm^2) which were meticulously weighed and immersed in 1.0 mL of a 5.0 μM solution of *Humicola insolens* cutinase (HiC, Novozym® 51032) in 0.1 M KPO buffer (pH = 8.0). The experiments were carried out at physiological temperature (*i.e.* 37 °C), with each polymer film undergoing analysis on to ensure the robustness of the results. After the degradation process, the specimens were washed with

MilliQ water and dried in a vacuum oven at room temperature until constant weight was reached. Mass loss data for each specimen were collected after 0.5, 1, 2, 4, 6, 24, 48, 72, 120 and 168 h.

2.6. Retention and release tests

Retention and release tests were carried out on the film consisting of neat PLA (m_PLA) and the film containing the alcoholysis product obtained with a 10 wt% of pentaerythritol (m_PLA_PE10).

Specimens of approximately 0.5 × 1.0 cm^2 were cut from each film and dried under vacuum until a constant weight was reached. The samples were immersed in 5.0 mL of an aqueous solution of pararosaniline hydrochloride at a concentration of 2.0 μg/mL. Pararosaniline hydrochloride (PARA) was selected as a model organic dye to mimic the behaviour of pharmaceutical compounds or pollutants. The tests were performed at 37 °C, *i.e.* the physiological temperature. After 24 h, the supernatant was analysed via UV-Vis spectrometry, using a Shimadzu® UV 1800 UV-Vis spectrometer. A calibration curve was constructed using standard solutions at different concentrations by measuring their absorbance at 539 nm. To determine the amount of dye retained by our formulations, Equation (5) was applied.

$$Absorbance\ [a.u.] = 0.21758 \cdot Concentration\ \left[\mu g\, mL^{-1}\right] + 0.02848 \qquad (5)$$

$$R^2 = 0.99769$$

To investigate the ability of the films to release the dye in a controlled manner over time, the loading of pararosaniline hydrochloride was performed as described above, using an aqueous solution at a concentration of 20.0 μg/mL. This higher concentration was selected to ensure adequate sensitivity of the UV-Vis determination. We evaluated the release capacity in 5.0 mL of MilliQ water at 37 °C, and the amount of dye released by the films was monitored for one week by performing UV-Vis analysis of the supernatant.

2.7. Water uptake measurements

The water uptake (WU) of films was assessed by immersing individual film disks (n = 3), accurately dried under vacuum, in Milli-Q water at room temperature. At predetermined time intervals, the samples were removed, gently blotted to remove surface water, and weighed. The amount of water retained at a certain time was calculated using Equation (6).

$$WU\ [\%] = \frac{w_t - w_0}{w_0} \cdot 100 \qquad (6)$$

Where w_t and w_0 are the weight of the soaked samples after time *t* and the initial weight of the dry film, respectively.

2.8. Cell viability evaluation

Human neuroblastoma SH-SY5Y cells were cultured in T75 flasks and maintained at 37 °C in a humidified incubator with 5.5% CO_2 in neuroblastoma medium based on DMEM/F-12 (Gibco, Thermo Fisher, Cat. 11320074) supplemented with 10% fetal bovine serum (FBS; Gibco, Thermo Fisher, Cat. 10270106), 1% Penicillin-Streptomycin (Gibco, Thermo Fisher, Cat. 15140122), and 1% GlutaMAX (Gibco, Thermo Fisher, Cat. 35050038). The culture medium was replaced twice a week during the growth process. Once 80% confluence was reached, SH-SY5Y cells were washed with sterile phosphate-buffered saline (PBS), trypsinized, and centrifuged at 1200 rpm for 5 min. For the cell viability evaluation, the cells were plated at a density of 3 × 10^5 cells per well in 6-well plates. After 24 h, the cells were exposed to the different samples for 24 h, 48 h, and 7 days.

Before exposure to the cell cultures, all PLA samples were sterilized by immersion in 70% ethanol for 30 min. They were then washed in ddH_2O three times for 10 min each and subsequently immersed in culture medium for 24h. After this preparation step, the samples were ready for use in the experiments. Cell cultures that were not exposed to the samples were used as controls.

For the cell viability evaluation, an MTT assay was performed. The cells were washed with Dulbecco's Phosphate-Buffered Saline (DPBS, Gibco) and incubated for 4 h at 37 °C with a 5 mg/mL solution of Thiazolyl Blue Tetrazolium Bromide (Sigma, Cat. No. M2128) dissolved in DPBS, under sterile conditions. Following incubation, the MTT solution was removed, and isopropanol (RS Pro) was added to each well to dissolve the formazan crystals. To achieve complete solubilization, an additional incubation step of 1 h was performed. Absorbance measurements were performed at 570 nm using a Cary 60 UV-Vis spectrophotometer (Agilent Technologies).

2.9. Recycling of the solvent

To investigate the potential for recycling Cy, approximately 70 mL of the aqueous mixture derived from the coagulation bath of the film preparation process was transferred to a round-bottomed flask. A short-path distillation setup equipped with a Vigreux column was connected to the boiler, followed by a Y-connector, a thermometer, a Liebig condenser, and a collecting flask. The mixture was first distilled at ambient pressure, collecting the fraction boiling up to 100 °C, which consisted mainly of water, thereby leaving a higher-boiling fraction enriched in crude Cyrene. After complete water removal, the remaining fraction in the boiler was recovered by vacuum distillation, reducing the pressure to 10 mbar and collecting the liquid distilled at around 110 °C. The recovered Cy fraction was subjected to 1H NMR analysis and compared to fresh Cy to confirm its composition.

3. Results and discussion

3.1. Study of the alcoholysis reaction

The alcoholysis reaction of PLA, carried out in the same solvent system used to produce porous films, was studied by evaluating both its progress over time through viscosimetric measurements and the influence of the amount of polyalcohol on the final properties of the products obtained by applying the optimized conditions. As previously mentioned, a solvent from renewable sources, namely Cy, was chosen together with environmentally friendly reagents, *i.e.* PE as polyalcohol and Zn stearate as a catalyst, both soluble in Cy as starting PLA. Three different polyalcohol concentrations with the same amount of catalyst were used, namely 2, 5 and 10 wt%.

3.1.1. Investigation of the reaction mixture viscosity

The kinetics of the alcoholysis reaction have not been investigated in detail, as this would require the use of different reactants, such as simplified model substrates (e.g., linear monohydric alcohols and methyl esters) [38]. Moreover, the viscosity of polymer solutions, especially at higher concentrations, may significantly influence reaction kinetics [18]. Indeed, monitoring viscosity over time may provide an indirect indication of reaction progress.

The viscosity of the reaction mixtures was analysed over time (after 24, 48 and 72 h) at 100 °C, *i.e.* at the temperature chosen to allow complete polymer solubilization and at which the alcoholysis processes were carried out. It was not possible to determine the viscosity of the mixtures at time zero as the polyalcohol dissolves during and as a result of the reaction. Viscosity values with a small deviation are obtained after about 24 h, so that this time represents a kind of initial value. Nevertheless, it is interesting to compare the viscosity values of the three formulations analysed, listed in Table 1, with that of the PLA solution in Cy at the concentration used in the mixtures, *i.e.* 20% w/v. It was found that the measured viscosity, which is 234 ± 4 mPa·s and constant over time, is significantly higher than that of the PLA/polyalcohol/catalyst

Table 1
Viscosities of the reaction mixtures (PLA_PE2, PLA_PE5 and PLA_PE10) over time at 100 °C.

Sample code	$\eta_{(24h)}$ [mPa·s]	$\eta_{(48h)}$ [mPa·s]	$\eta_{(72h)}$ [mPa·s]
PLA_PE2	93 ± 2	54 ± 0.5	49 ± 2
PLA_PE5	52 ± 0.4	29 ± 1	26 ± 1
PLA_PE10	28 ± 0.3	27 ± 2	25 ± 2

systems. This phenomenon may be related to the presence of the polyalcohol, a low molecular weight compound, but also to the alcoholysis reaction, which can cause a breaking of the macromolecular chains and therefore a decrease in the viscosity of the system.

Indeed, the dependence of viscosity on polyalcohol amount is evident for the three formulations after 24 h, with values decreasing almost linearly with the polyol amount, being 93 mPa·s, 52 mPa·s, and 28 mPa·s for PLA_PE2, PLA_PE5, and PLA_PE10, respectively. With increasing the reaction time, a significant decrease in viscosity was observed only for the systems with 2 and 5 wt% polyalcohol, from 93 to 54 and from 52 to 29 mPa·s for PLA_PE2, and PLA_PE5, respectively. This decrement was attributed to the alcoholysis reaction, which causes a reduction in the macromolecular weight through a transesterification reaction, as the composition of the mixture remained unchanged. The behaviour of the mixture with the highest PE content deserves further analysis. In contrast to the formulations with 2 and 5 wt% PE, the viscosity of PLA_PE10, remains stable during the three time periods analysed. Conversely, for PLA_PE2 and PLA_PE5, an almost constant value was reached only after 48 h, with a higher value of about 50 mPa·s for the formulation with 2 wt% PE, *i.e.* PLA_PE2. These results can be attributed to several factors. Indeed, in addition to the solubility limit of PE in the reactive system, the fact that the reactivity of the branched compound, formed as a result of the alcoholysis reaction, may be limited by steric factors that hinder subsequent transesterification processes must also be taken into account, as shown in other works [39]. Although the results obtained are only preliminary, they evidence not only the effectiveness of the conditions used for the alcoholysis reaction, but also that a reaction time of at least 48 h is required to achieve the formation of compounds with a constant molecular weight.

3.1.2. *Characterization of the alcoholysis products*

To better identify the chemical structure of the products obtained by the alcoholysis process, the samples prepared using optimized conditions, *i.e.* with a reaction time of 72 h, and precipitated in deionised water, were characterized by ^{1}H NMR. The NMR spectra of the formulations prepared from the three polyalcohol concentrations, namely PLA_PE2, PLA_PE5, and PLA_PE10, were compared with those of the linear, high molecular weight starting PLA (Fig. 2c).

As shown in Fig. 2c and widely reported, the spectrum of neat PLA exhibits two characteristic signals, labelled *a* and *b*, associated with protons of the repeating PLA unit [40–42]. The signal *a* (multiplet, C<u>H</u>) at 5.17 ppm was assigned to the methine proton, while the signal *b* (multiplet, C<u>H</u>$_3$) at 1.57 ppm was attributed to the methyl group. A further signal at 4.35 ppm (labelled *a'*), corresponding to the proton of the terminal methine, was barely detectable due to low concentration of terminal groups of the high molecular weight PLA.

The spectra of the alcoholysis products, namely PLA_PE2, PLA_PE5, and PLA_PE10, exhibited the typical signals of the repeating PLA unit as previously described at 5.17 ppm (*a*, multiplet, C<u>H</u>) and 1.57 ppm (*b*, multiplet, C<u>H</u>$_3$). In addition, signals at 4.35 ppm (*a'*, quadruplet, PLA-C<u>H</u>-OH) and 1.49 ppm (*b'*, multiplet, C<u>H</u>$_3$) were detected, associated to the terminal methine and terminal methyl protons, respectively. The presence of these signals is consistent with a high concentration of

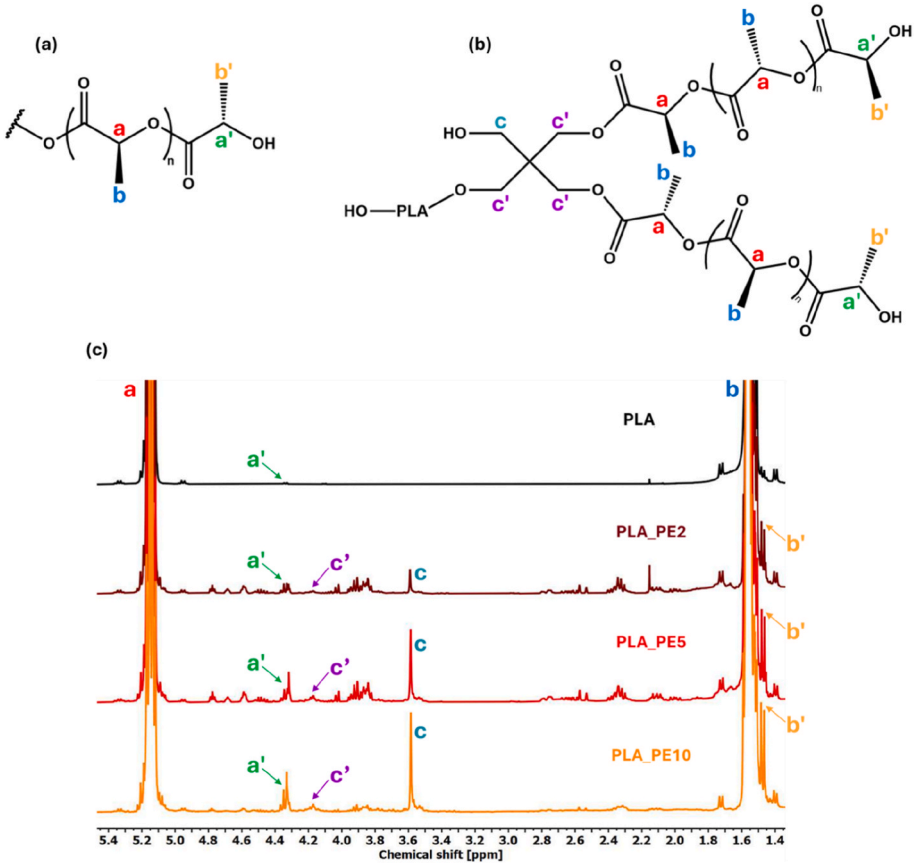

Fig. 2. (a) Structure of PLA, (b) structure of a branched compound obtained via the alcoholysis reaction of linear high-molecular-weight PLA and PE, (c) ^{1}H NMR spectra of neat PLA and PLA_PE2, PLA_PE5 and PLA_PE10.

terminal groups, thus confirming a decrease in molecular weight of the above compounds compared to the original PLA. Moreover, peaks at 4.19 ppm (*c'*, multiplet, PE-C<u>H</u>$_2$-*O*-PLA) and 3.61 ppm (*c*, singlet, PE-C<u>H</u>$_2$–<u>OH</u>) were detected, assigned to the methylene protons of PE arms functionalized with PLA and the methylene protons of PE with free OH groups, respectively. Since all the alcoholysis products were purified with deionised water to remove unreacted PE, the presence of peak *c* in all the samples can be attributed exclusively to PE that partially reacted with PLA and still exhibited free OH groups. This finding indicates that the PE remaining in the reaction mixture was only partially involved in the transesterification with PLA, resulting in a fraction of its OH groups not being converted. As shown in Fig. 2b, these results evidence the formation of branched structures characterized by arms functionalized with PLA chains and others with free hydroxyl groups. Although the end groups of pentaerythritol initially exhibit equivalent reactivity due to their chemical equivalence, the residual OH groups become increasingly sterically hindered as the alcoholysis proceeds due to the transesterification reactions with the PLA ester bonds. As a result, their reactivity decreases over time. This phenomenon has been demonstrated in several studies, which found a decrease in both the rate and the reactivity of the OH end groups in various polyalcohols - including the one used in the present work - as the steric hindrance around the core increases [39,43–45].

The molecular weight of the products derived from the alcoholysis reaction was determined from specific signals in the NMR spectra, using Equation (1); the results obtained are summarized in Table 2.

As previously reported, the linear starting PLA had a molecular weight of about 90000 g/mol [18]. The M_n of the three alcoholysis products resulted to be much lower than that of the starting polymer, being 5300, 2300 and 2000 g/mol for PLA_PE2, PLA_PE5 and PLA_PE10, respectively. The above findings, which are consistent with the viscosity measurements, once again demonstrate the effectiveness of the transesterification reaction in reducing the molecular weight of the polymer. Furthermore, a comparison of the behaviour of the three developed systems shows that the sample produced from 2 wt% PE has about twice as high M_n as the samples PLA_PE5 and PLA_PE10, which were both characterised by a similar M_n of about 2000 g/mol. As already mentioned in the results of the viscosity measurements, a kind of PE reactivity limit can be assumed.

In this regard, it is worth underlining that the sample treated for the same time and with 5 wt% PE without adding the catalyst to the reaction mixture, exhibited a spectrum that almost matched that observed for neat PLA (Fig. S1). Specifically, while peaks *a* and *b*, associated with the repeating unit of PLA, were clearly visible, peak *a'*, associated with terminal methine protons, was weak and difficult to detect, suggesting a low number of terminal groups, as previously observed for PLA. In addition, peak *c'* assigned to the protons of PE arms functionalized with PLA was undetectable, while peak *c* associated with the protons of PE arms with OH terminal groups was very weak. As this was precipitated like the other samples tested and washed with deionised water prior to the ^{1}H NMR measurement to remove the unreacted PE from the system, the lower intensity of *c* and *c'* indicates that almost all of the added polyalcohol did not react with PLA and was therefore removed during the washing steps. These results demonstrate that in the absence of catalyst, the extent of reaction between PE and PLA was negligible, highlighting the crucial role of this component in promoting the transesterification reaction between the hydroxyl groups of PE and the PLA ester bonds. In this context, it is worth underling that although Zn-based catalysts, such as Zn acetate, were used in the PLA alcoholysis [46,47], in this work for the first time Zn stearate and a new solvent system, namely Cy, were used. Although a detailed kinetic study was not undertaken due to the intrinsic complexity of applying kinetic models to a macromolecular polymeric system undergoing partial transesterification, the results obtained clearly demonstrate that the Cy/Zn stearate system can effectively promote the alcoholysis reaction, as evidenced by the significant reduction in PLA molecular weight and the formation of functionalized branched oligomers. Moreover, these findings indicate that the use of Cy as a solvent does not negatively affect the catalytic activity of zinc stearate, suggesting its potential applicability in the development of alternative sustainable catalytic systems.

Table 2
Degree of polymerization and molecular weight values for alcoholysis products.

Sample code	$A_{(a)}$[a] [a.u.]	DP	M_n [g/mol]
PLA_PE2	73	74	5300
PLA_PE5	31	32	2300
PLA_PE10	27	28	2000

[a] By considering $A_{(a')} = 1$.

The thermal properties of the alcoholysis products were analysed using a differential scanning calorimeter (DSC) and thermogravimetric analysis (TGA). The thermograms for the neat PLA and the oligomers obtained by alcoholysis reactions are shown in Fig. 3, while Table 3 contains a detailed summary of the extrapolated data.

PLA used in this study exhibited the typical behaviour of an amorphous polymer, as evidenced by the presence of an exothermic peak corresponding to cold crystallization, followed by an endothermic peak indicative of melting, characterized by equal enthalpy values. The alcoholysis products also exhibited thermal behaviour indicative of their amorphous nature, with comparable enthalpy values associated with cold crystallization (ΔH_{cc}) and melting (ΔH_m). However, the temperatures associated with these transitions differed from those determined for neat PLA. Indeed, both the cold crystallization (T_{cc}) and melting temperatures (T_m) of the alcoholysis products were shifted to lower values compared to neat PLA, phenomenon which can be ascribed to a reduction of their molecular weight. It is also interesting to note that ΔH_m and ΔH_{cc} of PLA_PE2 are much higher than those of neat PLA, the former being about 7 J/mol and that of PLA less than 1 J/mol, and higher than those of systems based on 5 and 10 wt% PE. This result could be related to the peculiar structures of the oligomers formed after the alcoholysis reaction. As described in other works, it can be inferred that a low PE content favours more linear structures with low branching while more branched compounds obtained with higher PE concentrations tend to hinder structuring [48,49].

Regarding the glass transition temperature (T_g), the DSC trace of neat PLA showed a T_g of about 60 °C, which is consistent with the values reported in the literature [50,51]. The samples which were subjected to the alcoholysis reaction had a T_g that is approx. 20 °C lower than that of neat PLA. Again, the different thermal behaviour of the oligomers compared to the pristine polymer can be attributed to their lower molecular weight and their peculiar, branched structure resulting from the alcoholysis process, which promotes the chain mobility and free volume.

For neat PLA, the TGA analysis showed an onset degradation temperature (T_{onset}) of ca. 350 °C and a maximum degradation rate (T_{max}) at ca. 400 °C. In the case of the alcoholysis products, the already proven reduction in molecular weight leads to a decrease in the two temperatures mentioned above, with no significant differences among the three samples. It is worth underlining that, despite their lower thermal stability compared to the neat polymer, the oligomers still have acceptable degradation temperatures, which makes them suitable for high-temperature processes.

3.2. Characterization of porous films

3.2.1. Investigation of the viscosity of the solutions used to prepare the films and their porosity

The additives, produced under optimal conditions, were used in the development of porous films by adding virgin PLA directly to the reaction mixture, containing the branched oligomers. Systems prepared from three different amounts of PE were exploited in a ratio 80/20 w/w respect to the high molecular weight PLA, maintaining a final concentration of 20% w/v of the dissolved polymer in Cy.

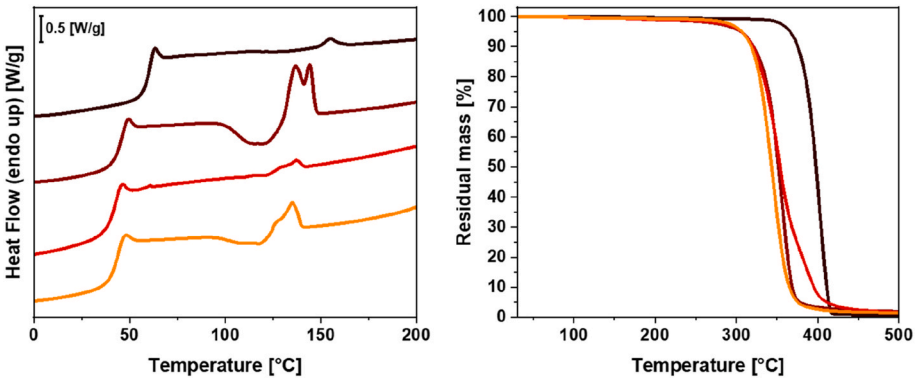

Fig. 3. DSC thermograms for the second heating phase (left) and TGA curves (right) for PLA (black), PLA_PE2 (maroon), PLA_PE5 (red) and PLA_PE10 (orange). (For interpretation of the references to color in this figure legend, the reader is referred to the Web version of this article.)

Table 3
Thermal properties of neat PLA and alcoholysis products.

Sample	T_g [°C]	T_{cc} [°C]	ΔH_{cc} [J/g]	T_m [°C]	ΔH_m [J/g]	T_{onset} [°C]	T_{max} [°C]
PLA	60	133	−0.54	155	0.70	351	404
PLA_PE2	46	118	−6.3	135/144	7.0	267	355
PLA_PE5	42	122	−0.41	137	0.60	273	353
PLA_PE10	43	120	−1.2	135	1.5	285	346

T_g = glass transition temperature; T_{cc} = cold crystallization temperature; ΔH_{cc} = cold crystallization enthalpy; T_m = melting temperature; ΔH_m = melting enthalpy; the enthalpy values were calculated on the assumption that the enthalpy of fusion for a completely crystalline PLA is equal to 93 J/g.
T_{onset} = temperature at which a weight loss of 2% was recorded; T_{max} = temperature at which the maximum rate of the degradation process occurs, obtained from DTG curves.

Viscosity measurements were carried out both on the solution based on neat PLA and on those containing the alcoholysis products, as the above parameter can directly influence the film porous structure. These measurements were carried out at 100 °C, *i.e.* the temperature used for film production, with shear rates from 10 to 100 s^{-1}; the results are given in Table 4.

Regarding neat PLA-based film, a direct comparison with the literature is challenging, as, to the best of our knowledge, no previous studies have investigated the viscosimetric behaviour of PLA solutions in Cy at 100 °C.

The results show a slight decrease in viscosity for m_PLA_PE2, while the decrease was more significant for m_PLA_PE5 and m_PLA_PE10, with both systems exhibiting a similar viscosity of approximately 120 mPa·s. The reduction observed in these samples is attributable to the incorporation of oligomers which, being characterised by a lower molecular weight than the matrix, tended to reduce the viscosity of the mixture, as reported for other systems [49,52,53]. Nevertheless, the reduction was limited due to their low concentration, *i.e.* 20 wt%. Furthermore, it is worth underlining that the observed trend is comparable to that found in the viscosimetric analyses of the oligomers, for which a similar viscosity was obtained for the m_PLA_PE5 and m_PLA_PE10 samples.

The porosities of the films obtained from PLA-based solutions calculated using Equation (2) and reported in Table 4, showed nearly constant values for all the systems investigated. To explain this result, it is important to consider that in the applied technique the main factor governing the porosity as well as pore morphology is the exchange kinetics between solvent and non-solvent [54,55], which in turn can be affected by several variables such as temperature and viscosity. Considering the latter parameter, noticeable variations in porosity are expected only when solutions with extremely different viscosities are used [56], thus explaining the limited influence of viscosity on the structure of the developed films.

Table 4
Viscosity of polymer solutions and porosity of the developed films.

Sample	Viscosity of the starting solution [mPa·s]	Porosity [%]
m_PLA	234 ± 4	89 ± 0.4
m_PLA_PE2	192 ± 2	87 ± 0.7
m_PLA_PE5	120 ± 1	90 ± 0.6
m_PLA_PE10	122 ± 1	89 ± 0.5

3.2.2. *Study of the film morphology*

In order to evaluate the influence of the branched oligomers on the resulting morphology, FE-SEM analysis was performed on neat PLA-based film and on films containing the additives. Fig. 4 shows the micrographs of the cross-sections, which provide an insight into the structural features of the analysed samples.

To better explain the creation of the porous structure, it is worth discussing its formation mechanism [57]. Film formation by phase inversion typically begins with a homogeneous, thermodynamically stable polymer solution. When the cast polymer solution is brought into contact with a liquid phase containing a non-solvent (NIPS), a new equilibrium point is established within the miscibility gap of the system. The thermodynamic state of the system then shifts toward this new equilibrium, entering a metastable region where phase separation occurs, leading to the formation of a polymer-rich phase and a polymer-lean phase, which rapidly separate. Both phases subsequently undergo coarsening, and the polymer-rich phase ultimately solidifies, thereby locking in the interpenetrating two-phase morphology. In particular, the leaf-like morphology, observed in the neat PLA film (Fig. 4a) is consistent with the findings of Milescu et al., [58] who applied the NIPS technique using the same solvent/non-solvent pair, *i.e.* Cy/water, and reported that this peculiar morphology results from to the rapid solvent/non-solvent exchange. The incorporation of the alcoholysis products into PLA matrix did not result in any appreciable morphological variations (Fig. 4b–d). This observation is consistent with the porosity data discussed above, confirming that, under identical processing conditions, pore formation is primarily governed by the solvent/non-solvent exchange process more than solutions viscosity.

It is worth underlining that, despite the highly porous structure and the presence of additives, the handling of the developed films is not limited (Fig. S2).

Another noteworthy finding from this analysis is the homogeneity exhibited by the developed systems. Indeed, high magnification images of both the cross-section (Fig. S3) and the dense surface (Fig. S4) revealed no evidence of aggregates or distinct domains of the branched oligomers. This finding confirms the effectiveness of the NIPS technique in ensuring a uniform dispersion of additives within the matrix, previously reported in several studies [20,59], and indicate good

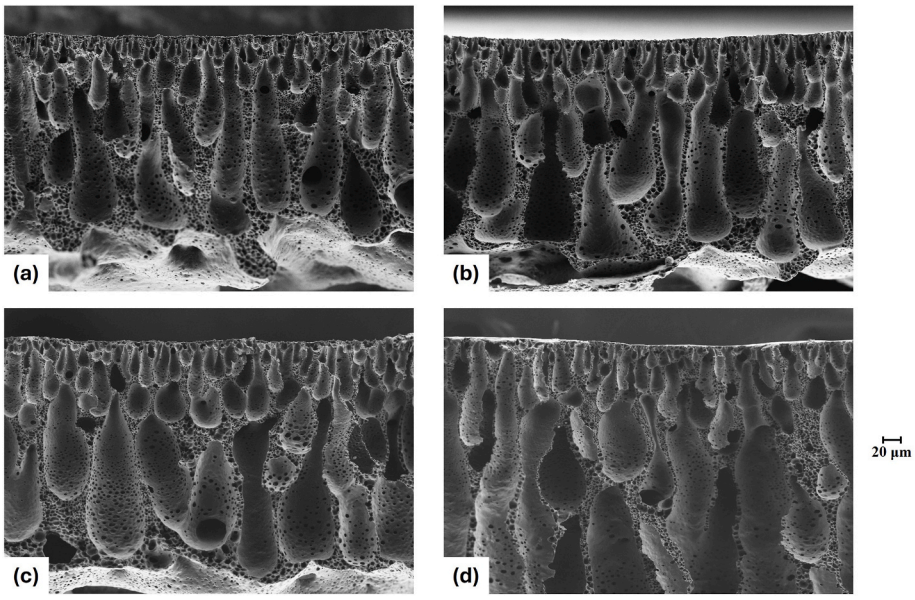

Fig. 4. FE-SEM micrographs of the cross-section of: (a) m_PLA, (b) m_PLA_PE2, (c) m_PLA_PE5, (d) m_PLA_PE10.

compatibility and miscibility between the alcoholysis products and the PLA matrix. Another interesting feature of the prepared films is their mechanical stability over time, as demonstrated by the retention of flexibility and physical integrity, which indicates good structural stability, as shown by photographs of the m_PLA_PE10 film aged for approximately one year (Fig. S5). The same behaviour was observed in the other developed films. Furthermore, chemical stability is confirmed by the complete overlap of the IR spectra of the pristine and aged samples (Fig. S6).

3.2.3. Study of film thermal properties

The films based on neat PLA and the PLA/oligomer mixture were characterised in terms of thermal properties using DSC and TGA analysis. The thermograms are shown in Fig. 5, while thermal data are listed in Table 5.

The neat PLA film exhibited thermal behaviour typical of its amorphous nature, with a cold crystallization peak (exothermic) followed by a melting peak (endothermic), both characterized by nearly identical enthalpy values. The same behaviour was observed for films containing the additives, which also showed equivalent ΔH_{cc} and ΔH_m values. Apart from the sample m_PLA_PE10, the incorporation of the alcoholysis products did not significantly affect the cold crystallization (T_{cc}) melting (T_m) and glass transition (T_g) temperatures compared to m_PLA, whose T_g of 57 °C was consistent with previously reported values [60]. In the case of m_PLA_PE10, the effect of the additive on the thermal properties of the film was more pronounced, as evidenced by a slight decrease in T_g, an increase in both ΔH_{cc} and ΔH_m, and a decrease in T_{cc}, indicating enhanced polymer structuring compared to neat PLA. This behavior can be attributed to a possible nucleating effect of the additive, which, due to its more highly branched structure compared to PLA_PE2 and PLA_PE5, exhibited a greater tendency towards aggregation and the formation of nanodomains. Although these nanodomains are not detectable by SEM, they are likely capable of promoting the structuring of the polymer matrix.

Table 5
Thermal properties of neat PLA-based film (m_PLA) and films containing alcoholysis products.

Sample	T_g [°C]	T_{cc} [°C]	ΔH_{cc} [J/g]	T_m [°C]	ΔH_m [J/g]
m_PLA	57	129	−5.1	154	5.0
m_PLA_PE2	57	128	−7.2	153	7.1
m_PLA_PE5	57	128	−5.7	152	6.0
m_PLA_PE10	52	117	−20	142/150	20

T_g = glass transition temperature; T_{cc} = cold crystallization temperature; ΔH_{cc} = cold crystallization enthalpy; T_m = melting temperature; ΔH_m = melting enthalpy; the enthalpy values were calculated on the assumption that the enthalpy of fusion for a completely crystalline PLA is equal to 93 J/g.

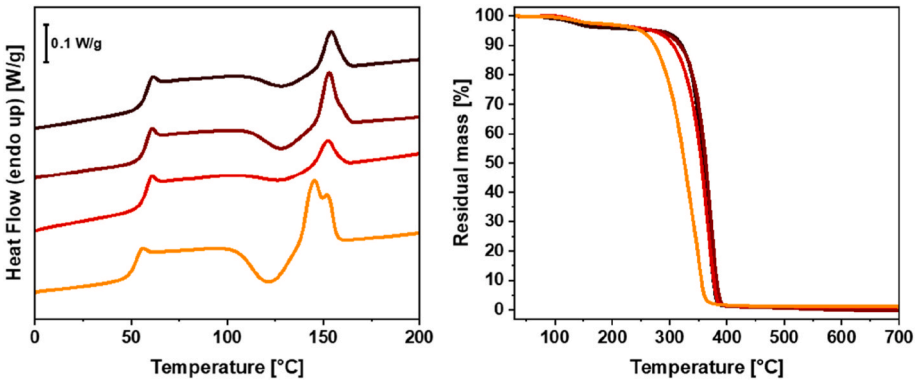

Fig. 5. DSC thermograms for the second heating phase (left) and TGA curves (right) for m_PLA (black), m_PLA_PE2 (maroon), m_PLA_PE5 (red) and m_PLA_PE10 (orange). (For interpretation of the references to color in this figure legend, the reader is referred to the Web version of this article.)

3.3. Enzymatic hydrolysis of the films

Enzymatic hydrolysis tests were carried out to assess the hydrolytic stability of the developed films, with particular attention to the role of the additives. The experiments were performed at 37 °C, using *Humicola insolens* cutinase (HiC) and KPO as the medium. The selection of the above enzyme was supported by several studies describing HiC as one of the most effective enzymes for polyester hydrolysis [61–63]. The temperature was chosen because it is the standard operating temperature used in enzymatic tests on various polyesters, including PLA, when physiological conditions are to be simulated [64,65]. The same measurements were performed by immersing the films in buffer without enzyme to distinguish pure hydrolytic degradation from enzymatically catalysed degradation. For all the systems studied, no weight loss was detected during the time range examined in the enzymatic hydrolysis analysis. The results of the enzymatic hydrolysis tests, calculated as percentage weight loss (WL) versus time, are shown in Fig. 6 and Fig. S7.

Fig. 6 shows the data of the measurements taken after one day of immersion of films within the enzyme-containing solutions, since the results evidenced considerable fluctuations at shorter times. Thus, considering the trend shown in Fig. 6 in detail, the presence of the additive appears to have a significant influence on the kinetics of the degradation process. While the neat PLA film and the sample containing PLA_PE2 exhibited a similar behavior after one day of treatment, with a weight loss of about 15 %, the PLA_PE5 and PLA_PE10 based systems showed a higher degradation, reaching 24 and 34 % for m_PLA_PE5 and m_PLA_PE10, respectively. The behavior of the tested systems after two days of treatment showed remarkable differences, as while the m_PLA and m_PLA_PE2 samples shared a similar behavior, reaching a weight loss of 36 and 47% respectively, the PLA_PE5 and PLA_PE10 based films exhibited a significant acceleration of the hydrolytic process, reaching a weight loss of around 80%. These results cannot be explained by considering the film morphologies, as these were quite similar, as the SEM measurements showed, but by considering the specific properties of the additives, and particularly their molecular weight, which influences the concentration of the end groups. As already reported, PLA_PE2 was characterized by a higher molecular weight compared to PLA_PE5 and PLA_PE10, reaching values of around 2000 g/mol under the conditions used to produce the films. This property directly influences the concentration of –OH groups present in the system, which increases by decreasing the molecular weight of the additive for the same amount. In addition, it is worth underlining that the branched geometry promoted by the alcoholysis reaction performed with the polyol also favors the formation of systems rich of hydroxyl groups and therefore their concentration in the mixture used for film preparation. In this context, several studies demonstrated the key role of the above-mentioned functionality in the degradation process of polyesters. Indeed, hydroxyl groups were introduced into polyesters to improve degradability. In a recent study [66], for example, the behavior of conventional polyesters, such as PCL and poly (11-hydroxyundecanoate) (PHU) was compared with that of a polymer bearing hydroxyl groups, namely poly (10, 11-epoxyundecanoic acid) (PEUA), finding that the hydroxyl groups had a positive effect on the degradability of the polyesters in both hydrolytic and enzymatic media. In another study [67], some hydroxy-functional copolyesters were synthesized from adipic acid, 1,8-octanediol and glycerol, whereby the hydroxyl groups concentration was modified by increasing the ratio of 1,8-octanediol to glycerol. The degradation measurements, investigated in phosphate buffer (pH ~ 7.4 at 37 °C) for a specific time, evidenced that the observed weight loss after 7 days ranged from 20%, for the polymers with an adipic acid:1,8-octanediol: glycerol ratio of 1:0.8:0.2 to 55% for polymers characterized by a higher glycerol concentration, demonstrating that the biodegradation rate increases with increasing hydroxyl content. This phenomenon was attributed to the combined effect of increased hydrophilicity, decreased crystallinity as well as to the catalytic effect of free hydroxyl groups, all of which promote the breaking of polymer ester bonds under hydrolytic conditions.

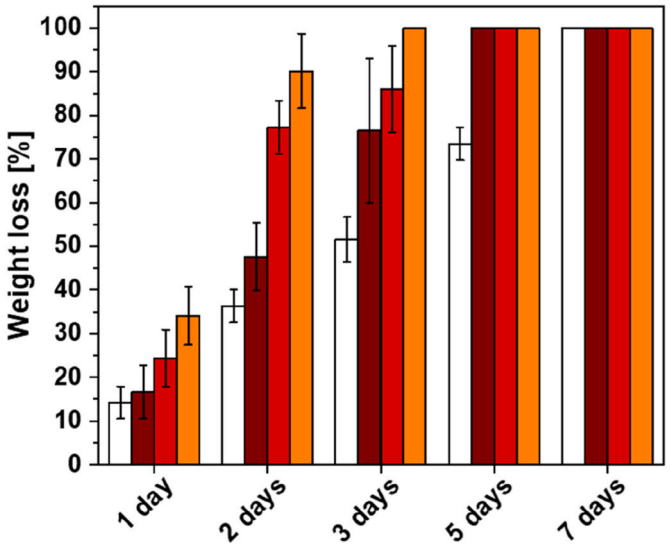

Fig. 6. Percentage of weight loss as a function of time, for m_PLA (white), m_PLA_PE2 (maroon), m_PLA_PE5 (red) and m_PLA_PE10 (orange). (For interpretation of the references to color in this figure legend, the reader is referred to the Web version of this article.)

After three days, the sample with PLA_PE2 also achieved a high weight loss, namely around 80 %, but its degradation kinetics was slower than that of the two other systems analysed, which had almost completely decomposed by this time. This result also seems to support the effect of the hydroxyl functionalities in the degradation of the polymer, as the PLA_PE2-based film was less rich in OH groups for the same amount of additive added to the mixture. Finally, all three films containing the branched additive were completely degraded after five days, while neat PLA sample was only degraded after seven days.

The results obtained of the enzymatic hydrolysis experiments demonstrate that the degradability of PLA-based films can be tuned by incorporating the developed additives which are highly compatible with the polymer matrix, and whose production is based on a simple and an environmentally friendly method, whereby the film preparation does not require separation of the compounds originating directly from PLA recycling.

3.4. Study of the film retention and release capacity

To evaluate the retention capacity of PLA-based films and the influence of the branched oligomers on this property, retention tests were performed with aqueous solutions of pararosaniline hydrochloride (PARA), a cationic organic dye which mimics the behaviour of amino-containing drugs. For this reason, this compound is suitable as a model for studying drug-polymer interactions [68]. In the retention tests, the neat PLA film and the film containing the oligomer obtained using the highest concentration of PE, namely m_PLA_PE10, were analysed. The experimental tests were carried out at 37 °C, *i.e.,* at the physiological temperature, and the resulting supernatants were analysed after 1 and 14 days of contact with the films using a UV-Vis spectrometer. The amount of dye retained by the films was calculated using Equation (5). The results are shown in Fig. 7a, which also includes photographs of the porous and dense surfaces of the films after exposure to the PARA solution.

After 24 h, the amount of retained dye was relatively low for both films, measuring 59 ± 18 μg/g for m_PLA and 65 ± 6 μg/g for m_PLA_PE10. After 14 days, m_PLA exhibited a modest increase, reaching 71 ± 6 μg/g, while m_PLA_PE10 showed a significant increase, achieving a retained dye value of 153 ± 13 μg/g. The variation in PARA

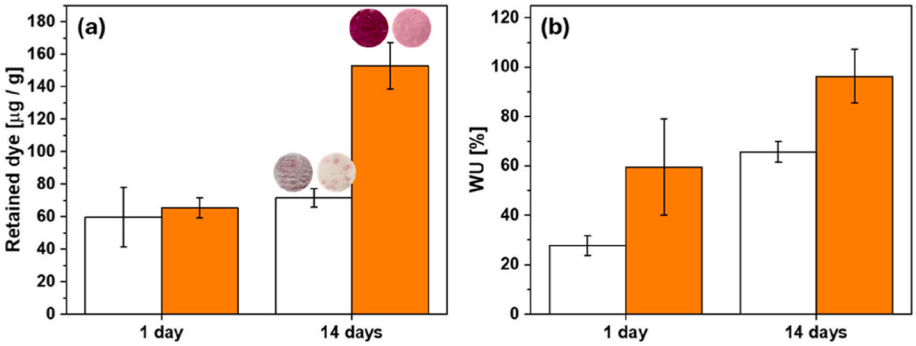

Fig. 7. (a) Retained PARA and (b) water uptake for m_PLA (white) and m_PLA_PE10 (orange). (For interpretation of the references to color in this figure legend, the reader is referred to the Web version of this article.)

uptake among the films was further confirmed by the discoloration observed on their surfaces after 14 days of exposure to the solution. The pure PLA film displayed a non-uniform pink color, whereas the m_PLA_PE10 film was characterized by a very uniform coloring, with the porous surface showing a more intense shade, suggesting that the larger surface area of the above-mentioned part of the film promoted dye retention.

Comparing the results of the analysis of the neat PLA film with those of the system containing the oligomer, the low affinity of the high molecular weight PLA for cationic molecules can be deduced, a phenomenon due to the limited number of functional end groups available for interactions. Indeed, it is possible to hypothesize that despite the large surface area provided by the porous structure of the film, the lack of functionality limits its retention capacity. In this context, it is worth underlining that several studies highlighted that the functionalization of PLA plays a crucial role in improving effective interactions with drugs, dyes or bioactive molecules, thereby increasing loading efficiency and affinity [69–71]. On the other hand, the incorporation of the branched oligomer into the system, which, as reported above, did not affect the porosity and morphology of films, led to an increase in the content of functional groups which can promote the adsorption of PARA thanks to non-specific interactions.

As the retention tests were carried out in aqueous solutions, films wettability must be taken into account to obtain a more comprehensive interpretation of the results. To this end, the water uptake (WU) was measured for both m_PLA and m_PLA_PE10. The WU values over time, calculated according to Equation (6), are reported in Fig. S8, while Fig. 7b shows the results obtained after 1 day and 14 days, corresponding to the time points of the retention tests. The neat PLA-based film exhibited a WU of 27 ± 4 % after 24 h, which increased to 65 ± 4 % after 14 days. In contrast, m_PLA_PE10 showed higher WU values after the same time, reaching 59 ± 18 % and 96 ± 10 % after 1 and 14 days, respectively. These results, which indicate that the water absorption capacity is increased by the introduction of the alcoholysis product characterized by the presence of hydroxyl terminal groups, are in agreement with the study by Singh et al., [72] who demonstrated that for PLA with molecular weight below 5000 g/mol, the presence of –OH end groups significantly increases the water retention. On this basis, it can be deduced that the presence of –OH groups resulting from the introduction of the additive promotes the uptake of the dye both through the specific interactions between the molecule and the above-mentioned functionalities. Moreover, the increase of the wettability of the film due to the polarity of the additive can favor the diffusion of the dye within the porous structure.

In addition, the ability of the films m_PLA and m_PLA_PE10 to release PARA in a controlled manner over time was investigated, as this is a key parameter for evaluating the strength and efficacy of dye-polymer interactions [73]. PARA loading was carried out using an aqueous solution at a concentration of 20 µg/mL, and the release capacity in MilliQ water at 37 °C was evaluated by UV-Vis analysis (Fig. 8).

A rapid initial release was observed for both films, with a burst in the first hours, followed by a gradual decrease in release rate until completion, which occurred after 7 days. Interestingly, after 5 min, while the neat PLA film, m_PLA, showed a cumulative release of approximately 86%, the sample containing the additive, m_PLA_PE10, exhibited a lower cumulative release of approximately 60%. Although both films eventually achieved complete release within one week, their release kinetics were markedly different: the average release rate for the neat PLA system was 0.015 $\mu g \cdot (mL \cdot h)^{-1}$, compared to 0.009 $\mu g \cdot (mL \cdot h)^{-1}$ for m_PLA_PE10, indicating a slower and more controlled release from the additive-containing film. As with other PLA-based systems, these results can be explained by the fact that the increased hydrophilicity caused by the presence of the branched oligomer tunes the release behavior of the film, further confirming the effectiveness of the developed materials [74,75]. Although these were preliminary tests, the release profiles observed are encouraging, as controlled release is a key prerequisite for biomedical and drug-delivery applications, allowing prolonged therapeutic action and avoiding frequent dosing [76]. Specifically, release profiles characterized by an initial burst followed by sustained delivery, similar to that of m_PLA_PE10, have been reported for PLA-based systems designed for the release of antibiotics and bacteriocins [77–79]. This peculiar release behaviour is particularly advantageous for antimicrobial applications, as the initial burst release can rapidly eliminate most of the pathogens, while the subsequent sustained

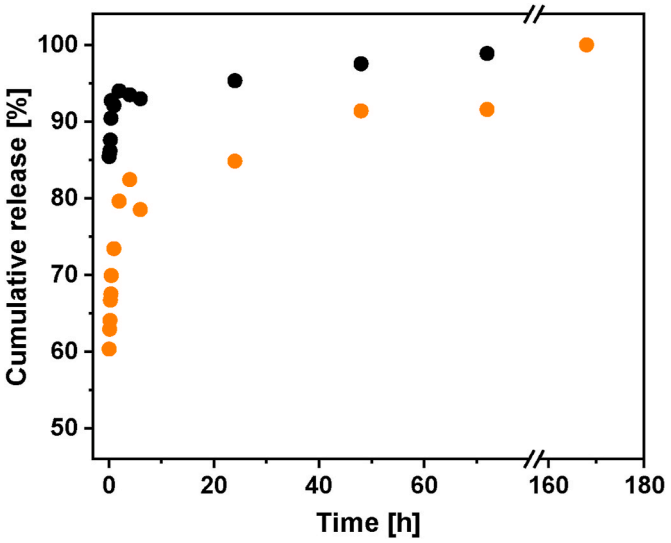

Fig. 8. Cumulative release over time for m_PLA (black) and m_PLA_PE10 (orange). (For interpretation of the references to color in this figure legend, the reader is referred to the Web version of this article.)

release helps to keep the infection under control over time [79].

3.5. Cell viability evaluation

The biocompatibility of the developed films was assessed using the human neuroblastoma cell line SH-SY5Y. Cell morphology and adhesion were initially observed with an optical microscope before exposure and after 2 and 7 days of exposure to the samples (Fig. S9).

The acquired images revealed no significant differences between the control system, consisting of cells cultured in the absence of films, and cells maintained in contact with the developed materials. Moreover, a qualitative increase in cell density was observed over time, suggesting normal proliferation from day 2 to day 7.

For quantity evaluation of cytotoxicity and cell viability, the MTT assay was performed after 7 days of exposure. This commonly used assay measures the metabolic activity of living cells through the reduction of (3-[4,5-dimethylthiazol-2-yl]-2,5 diphenyl tetrazolium bromide) to insoluble formazan crystals, which provides a reliable indication of cell viability [80]. Cell viability percentages, shown in Fig. 9, were calculated relative to untreated controls and were defined as the number of live cells divided by the total number of cells.

The results were very encouraging as all PLA-based systems, including those containing the additive, exhibited cell viability values above 100 %, indicating not only the absence of cytotoxic events but also successful cell proliferation over time. These findings are in agreement with previous studies demonstrating the biocompatibility of PLA and PLA-based composites for different cell phenotypes, including neuronal cells, fibroblasts and Chinese Hamster Ovary cell line [81–83]. Indeed, it was reported in the literature that lactic acid eventually released during PLA degradation can result in an increase in neural cell proliferation, which could be attributed to its ability to lower the intracellular redox state [84–86].

Moreover, this work demonstrated that the introduction of alcoholysis products does not compromise the intrinsic biocompatibility of the PLA matrix and may even support enhanced cellular growth.

3.6. Recycling of Cyrene®

With the aim of developing a PLA upcycling process in line with the principles of the circular economy, solvent recovery is a crucial step to minimize waste generation and reduce the environmental impact of polymer processing [87]. With this in mind, one objective of this work was to develop a “closed loop” approach, in which the solvent used both for the alcoholysis process and the preparation of polymer solutions for porous films could be recovered and reused for subsequent processing cycles. To this end, the mixture of Cy and water resulting from the application of the NIPS technique for film development was subjected to a distillation step. This process took advantage of the large difference in the boiling points of the two solvents [88,89], which are 100 °C for water and 227 °C for Cy, allowing selective evaporation of water and recovery of purified Cy. Moreover, Stini et al. specifically reported the possibility of recovering Cy by separating it from water via distillation, further supporting the approach adopted in the present work [90].

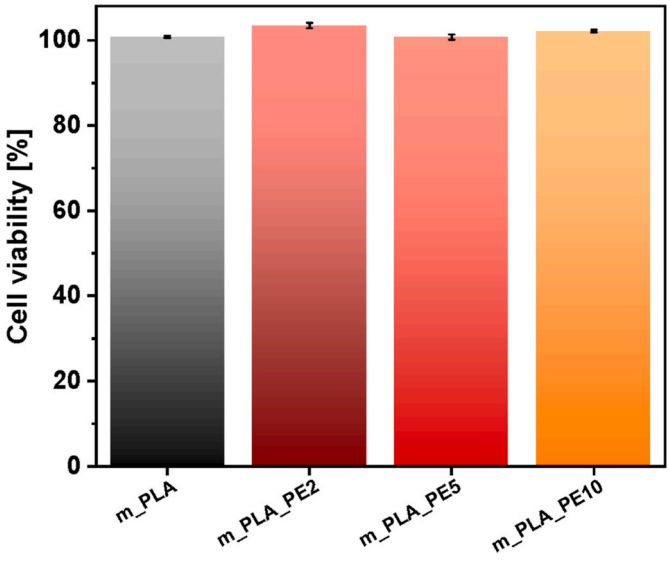

Fig. 9. Percentage of cell viability of SH-SY5Y by MTT assay.

After the distillation process, the residue collected from the boiler was analysed by ^{1}H NMR spectroscopy to assess the efficacy of the recovery procedure. The spectrum of the recovered Cy was compared with that of virgin Cy (Fig. S10), and the observed signals were assigned according to the work of Cseri et al., [91] who reported the chemical shifts of several bio-based solvents in $CDCl_3$, including Cy.

The spectrum of fresh Cy was consistent with the literature values, confirming the purity of the material employed [90,92]. The ^{1}H NMR spectrum of the recovered Cy showed no significant deviations from that of the original solvent, and no additional signals attributable to impurities or degradation products were detected. These findings demonstrate the efficiency of the distillation process in recycling Cy and confirm that the recovered solvent can be reused without loss of quality. The possibility to recover and reuse Cy without compromising its purity and chemical integrity represents a significant step toward the implementation of a robust, circular and environmentally friendly approach for PLA processing and upcycling.

4. Conclusion

In this work, a sustainable approach for upcycling polylactic acid was developed, along with a closed-loop method enabling the reuse of products derived from its chemical treatment. The reaction exploited – an easily scalable alcoholysis process performed in the green solvent dihydrolevoglucosenone (Cyrene®, Cy) with bio-based reagents such as pentaerythritol and zinc stearate – efficiently produced oligomeric products with a branched, highly functionalized structure. The closed-loop concept was validated by directly reusing the branched oligomers in the reaction medium, without any work-up, for the fabrication of porous films, as well as by recovering Cy after film preparation. The films, obtained by incorporating virgin polymer into the oligomeric mixture derived from the alcoholysis reaction to enhance processability, exhibited a characteristic leaf-like morphology resulting from the preparation method. Moreover, they displayed a high retention capacity for pararosaniline hydrochloride, a cationic organic dye, selected to mimic the behavior of amino-terminated drugs, a phenomenon attributed to the functional properties imparted by the branched additives. The developed films, which demonstrated biocompatibility and accelerated enzymatic hydrolysis compared to the neat polymer, could be used as controlled-release systems. Moreover, the overall process remained simple, low-impact, and scalable. These results highlight both the materials and the methodology as a promising advancement for sustainable PLA valorization.

CRediT authorship contribution statement

Martina Cozzani: Writing – original draft, Investigation, Formal analysis, Data curation. **Alessandro Fortunato:** Visualization, Investigation. **Giacomo Damonte:** Writing – review & editing, Visualization, Validation, Methodology, Investigation. **Alessandro Pellis:** Writing – review & editing, Validation, Funding acquisition. **Donatella Di Lisa:** Writing – review & editing, Validation, Investigation. **Laura Pastorino:** Writing – review & editing, Validation, Investigation. **Orietta Monticelli:** Writing – review & editing, Supervision, Methodology, Funding acquisition, Conceptualization.

Declaration of competing interest

The authors declare that they have no known competing financial interests or personal relationships that could have appeared to influence the work reported in this paper.

Acknowledgements

Funded by PLA-VIT project (P20229KM4Z) (European Union Next-Generation EU through the PRIN (Progetti di Ricerca di Rilevante Interesse Nazionale) PNRR (Piano Nazionale di Ripresa e Resilienza) 2022 call from the Italian Ministry of Education and Research (MUR)) and ERC CIRCULARIZE (101114664) (European Union). Views and opinions expressed are, however, those of the author(s) only and do not necessarily reflect those of the European Union or the European Research Council. Neither the European Union nor the granting authority can be held responsible for them.

Appendix A. Supplementary data

Supplementary data to this article can be found online at https://doi.org/10.1016/j.polymer.2026.129825.

Data availability

Data will be made available on request.

References

[1] T. Thiounn, R.C. Smith, J. Polym. Sci. 58 (10) (2020) 1347–1364, https://doi.org/10.1002/pol.20190261.
[2] P. van den Tempel, F. Picchioni, Recycling 10 (1) (2025) 1, https://doi.org/10.3390/recycling10010001.
[3] D. Briassoulis, A. Pikasi, M. Hiskakis, Crit. Rev. Environ. Sci. Technol. 49 (20) (2019) 1835–1892, https://doi.org/10.1080/10643389.2019.1591867.
[4] L. Ritzen, B. Sprecher, C. Bakker, R. Balkenende, Resour. Conserv. Recycl. 199 (2023) 107268, https://doi.org/10.1016/j.resconrec.2023.107268.
[5] J.-G. Rosenboom, R. Langer, G. Traverso, Nat. Rev. Mater. 7 (2022) 117–137, https://doi.org/10.1038/s41578-021-00407-8.
[6] J.D. Badia, A. Ribes-Greus, Eur. Polym. J. 84 (2016) 22–39, https://doi.org/10.1016/j.eurpolymj.2016.09.005.
[7] F. Vilaplana, S. Karlsson, Macromol. Mater. Eng. 293 (4) (2008) 274–297, https://doi.org/10.1002/mame.200700393.
[8] N. Mallegni, F. Cicogna, E. Passaglia, V. Gigante, M.-B. Coltelli, S. Coiai, Compounds 5 (1) (2025) 4, https://doi.org/10.3390/compounds5010004.
[9] C. Sun, Z. Huang, Y. Liu, C. Li, H. Tan, Y. Zhang, J. Polym. Environ. 28 (2020) 1315–1325, https://doi.org/10.1007/s10924-020-01688-w.
[10] F. Carrasco, P. Pagès, J. Gámez-Pérez, O.O. Santana, M.L. Maspoch, Polym. Degrad. Stabil. 95 (2) (2010) 116–125, https://doi.org/10.1016/j.polymdegradstab.2009.11.045.
[11] J.D. Badia, E. Strömberg, S. Karlsson, A. Ribes-Greus, Polym. Degrad. Stabil. 97 (4) (2012) 670–678, https://doi.org/10.1016/j.polymdegradstab.2011.12.019.
[12] M. Żenkiewicz, J. Richert, P. Rytlewski, K. Moraczewski, M. Stepczyńska, T. Karasiewicz, Polym. Test. 28 (4) (2009) 412–418, https://doi.org/10.1016/j.polymertesting.2009.01.012.
[13] B. Brüster, F. Addiego, F. Hassouna, D. Ruch, J.-M. Raquez, P. Dubois, Polym. Degrad. Stabil. 131 (2016) 132–144, https://doi.org/10.1016/j.polymdegradstab.2016.07.017.
[14] A.L. Merchan, T. Fischöder, J. Hee, M.S. Lehnertz, O. Osterthun, S. Pielsticker, J. Schleier, T. Tiso, L.M. Blank, J. Klankermayer, R. Kneer, P. Quicker, G. Walther, R. Palkovits, Green Chem. 24 (2022) 9428–9449, https://doi.org/10.1039/D2GC02244C.
[15] P. McKeown, M.D. Jones, Sustain. Chem. 1 (1) (2020) 1–22, https://doi.org/10.3390/suschem1010001.
[16] M. Niaounakis, Eur. Polym. J. 114 (2019) 464–475, https://doi.org/10.1016/j.eurpolymj.2019.02.027.
[17] R. Petrus, D. Bykowski, P. Sobota, ACS Catal. 6 (8) (2016) 5222–5235, https://doi.org/10.1021/acscatal.6b01009.
[18] G. Damonte, A. Vallin, L. Giribaldi, A. Pellis, M. Hakkarainen, S. Subramaniyan, P. Campaner, O. Monticelli, Sustain. Mater. Technol. 43 (2025) e01320, https://doi.org/10.1016/j.susmat.2025.e01320.
[19] S. Shi, X.H. Wang, G. Guo, M. Fan, M.J. Huang, Z.Y. Qian, Int. J. Nanomed. 24 (5) (2010) 1049–1055, https://doi.org/10.2147/ijn.s13169.
[20] M. Cozzani, P.F. Ferrari, G. Damonte, A. Pellis, O. Monticelli, Macromol. Biosci. 24 (12) (2024) 2400272, https://doi.org/10.1002/mabi.202400272.
[21] L. Gangolphe, C.Y. Leon-Valdivieso, B. Nottelet, S. Déjean, A. Bethry, C. Pinese, F. Bossard, X. Garric, Mater. Sci. Eng. C 129 (2021) 112339, https://doi.org/10.1016/j.msec.2021.112339.
[22] S. Chitrattha, T. Phaechamud, Mater. Sci. Eng., C 1 (58) (2016) 1122–1130, https://doi.org/10.1016/j.msec.2015.09.083.
[23] X. Zhou, G. Zhou, R. Junka, N. Chang, A. Anwar, H. Wang, X. Yu, Colloids Surf. B Interfaces 197 (2021) 111420, https://doi.org/10.1016/j.colsurfb.2020.111420.
[24] L. Valle, L. Maddalena, G. Damonte, F. Carosio, A. Pellis, O. Monticelli, Colloids Surf. B Biointerfaces 236 (2024) 113806, https://doi.org/10.1016/j.colsurfb.2024.113806.
[25] G. Damonte, R. Spotorno, D. Di Fonzo, O. Monticelli, ACS Appl. Polym. Mater. 4 (9) (2022) 6521–6530, https://doi.org/10.1021/acsapm.2c00923.
[26] Z. Xue, Z. Sun, Y. Cao, Y. Chen, L. Tao, K. Li, L. Feng, Q. Fu, Y. Wei, RSC Adv. 3 (2013) 23432–23437, https://doi.org/10.1039/C3RA41902A.
[27] M.W. Nugraha, M.D.H. Wirzal, F. Ali, L. Roza, N.S. Sambudi, J. Environ. Chem. Eng. 9 (5) (2021) 106033, https://doi.org/10.1016/j.jece.2021.106033.
[28] Y. Zhu, C. Gao, X. Liu, T. He, J. Shen, Tissue Eng. 10 (2004) 53–61, https://doi.org/10.1089/107632704322791691.
[29] J. Yang, Y. Wan, C. Tu, Q. Cai, J. Bei, S. Wang, Polym. Int. 52 (12) (2003) 1892–1899, https://doi.org/10.1002/pi.1272.
[30] Y. Lin, L. Wang, P. Zhang, X. Wang, X. Chen, X. Jing, Z. Su, Acta Biomater. 2 (2) (2006) 155–164, https://doi.org/10.1016/j.actbio.2005.10.002.
[31] T. Hirotsu, K. Nakayama, T. Tsujisaka, A. Mas, F. Schue, Polym. Eng. Sci. 42 (2) (2002) 299–306, https://doi.org/10.1002/pen.10949.
[32] G.-H. Koo, J. Jang, Fibers Polym. 9 (2008) 674–678, https://doi.org/10.1007/s12221-008-0106-1.
[33] X. Liu, T. Wang, L.C. Chow, M. Yang, J.W. Mitchell, Int. J. Polym. Sci. 1 (2014) 827028, https://doi.org/10.1155/2014/827028.
[34] N. Vicentini, T. Gatti, M. Salerno, Y.S. Hernandez Gomez, M. Bellon, S. Gallio, C. Marega, F. Filippini, E. Menna, Mater. Chem. Phys. 214 (2018) 265–276, https://doi.org/10.1016/j.matchemphys.2018.04.042.
[35] M.S. Alvarez Serafini, D.M. Reinoso, G.M. Tonetto, Energy 164 (2018) 264–274, https://doi.org/10.1016/j.energy.2018.08.182.
[36] P. Antony, S.K. De, Polymer 40 (6) (1999) 1487–1493, https://doi.org/10.1016/S0032-3861(98)00362-0.
[37] M. Abendrot, U. Kalinowska-Lis, Int. J. Cosmet. Sci. 40 (4) (2018) 319–327, https://doi.org/10.1111/ics.12463.
[38] M.E. Cucciolito, M. Lega, V. Papa, F. Ruffo, Catal. Lett. 146 (2016) 1113–1117, https://doi.org/10.1007/s10562-016-1733-6.
[39] F.M. Lamberti, L.A. Román-Ramírez, P. Mckeown, M.D. Jones, J. Wood, Processes 8 (6) (2020) 738, https://doi.org/10.3390/pr8060738.
[40] R. Itzinger, C. Schwarzinger, C. Paulik, J. Polym. Res. 27 (2020) 383, https://doi.org/10.1007/s10965-020-02339-3.
[41] J.L. Espartero, I. Rashkov, S.M. Li, N. Manolova, M. Vert, Macromolecules 29 (10) (1996) 3535–3539, https://doi.org/10.1021/ma950529u.
[42] K. Suganuma, H. Matsuda, H.N. Cheng, M. Iwai, R. Nonokawa, T. Asakura, Polym. Test. 38 (2014) 35–59, https://doi.org/10.1016/j.polymertesting.2014.05.018.
[43] M.V. Kopyshev, A.V. Khasin, T.P. Minyukova, A.A. Khassin, T.M. Yurieva, React. Kinet. Mech. Catal. 117 (2016) 417–427, https://doi.org/10.1007/s11144-015-0964-7.
[44] M.P.W. Hardhianti, Rochmadi, M.M. Azis, Processes 10 (1) (2022) 39, https://doi.org/10.3390/pr10010039.
[45] F.M. Lamberti, A. Ingram, J. Wood, Processes 9 (6) (2021) 921, https://doi.org/10.3390/pr9060921.
[46] E. Cheung, C. Alberti, S. Enthaler, ChemistryOpen 9 (12) (2020) 1224–1228, https://doi.org/10.1002/open.202000243.
[47] F.M. Lamberti, L.A. Román-Ramírez, A.P. Dove, J. Wood, Polymers 14 (9) (2022) 1763, https://doi.org/10.3390/polym14091763.
[48] J. You, L. Lou, W. Yu, C. Zhou, J. Appl. Polym. Sci. 129 (4) (2013) 1959–1970, https://doi.org/10.1002/app.38912.
[49] G. Damonte, M. Cozzani, M. Ozenda, C. Siracusa, M.J. Calandri, A. Pellis, G. M. Guebitz, O. Monticelli, Int. J. Macromol. 319 (2) (2025) 145457, https://doi.org/10.1016/j.ijbiomac.2025.145457.
[50] M. Cristea, D. Ionita, M.M. Iftime, Materials 13 (22) (2020) 5302, https://doi.org/10.3390/ma13225302.
[51] W.-J. Yin, M. Krack, X. Li, L.-Z. Chen, L.-M. Liu, Prog. Nat. Sci. Mater. Int. 27 (2) (2017) 283–288, https://doi.org/10.1016/j.pnsc.2017.03.003.
[52] H. Yang, J. Du, Molecules 29 (1) (2023) 169, https://doi.org/10.3390/molecules29010169.
[53] S. Yu, Y. Zhang, H. Hu, J. Li, W. Zhou, X. Zhao, S. Peng, RSC Adv. 12 (2022) 31629–31638, https://doi.org/10.1039/D2RA03513H.
[54] A.S.M. Wittmar, D. Koch, O. Prymak, M. Ulbricht, ACS Omega 5 (42) (2020) 27314–27322, https://doi.org/10.1021/acsomega.0c03632.
[55] X. Tan, D. Rodrigue, Polymers 11 (7) (2019) 1160, https://doi.org/10.3390/polym11071160.
[56] C. Kahrs, J. Schwellenbach, Polymer 186 (2020) 122071, https://doi.org/10.1016/j.polymer.2019.122071.
[57] J.T. Jung, J.F. Kim, H.H. Wang, E. di Nicolo, E. Drioli, Y.M. Lee, J. Membr. Sci. 514 (2016) 250–263, https://doi.org/10.1016/j.memsci.2016.04.069.
[58] R.A. Milescu, A. Zhenova, M. Vastano, R. Gammons, S. Lin, C.H. Lau, J.H. Clark, C. R. McElroy, A. Pellis, ChemSusChem 14 (16) (2021) 3367–3381, https://doi.org/10.1002/cssc.202101125.
[59] J. Zhang, M. Zheng, Y. Zhou, L. Yang, Y. Zhang, Z. Wu, G. Liu, J. Zheng, Membranes 12 (4) (2022) 386, https://doi.org/10.3390/membranes12040386.
[60] S. Farah, D.G. Anderson, R. Langer, Adv. Drug Deliv. Rev. 107 (2016) 367–392, https://doi.org/10.1016/j.addr.2016.06.012.

[61] R. Brackmann, C. de Oliveira Veloso, A.M. de Castro, M.A.P. Langone, 3 Biotech 13 (2023) 135, https://doi.org/10.1007/s13205-023-03555-6.
[62] Q. Huang, S. Kimura, T. Iwata, Biomacromolecules 24 (12) (2023) 5836–5846, https://doi.org/10.1021/acs.biomac.3c00835.
[63] S. Weinberger, K. Haernvall, D. Scaini, G. Ghazaryan, M.T. Zumstein, M. Sander, A. Pellis, G.M. Guebitz, Green Chem. 19 (2017) 5381–5384, https://doi.org/10.1039/C7GC02905E.
[64] M.E.E. Temporiti, L. Nicola, E. Nielsen, S. Tosi, Microorganisms 10 (6) (2022) 1180, https://doi.org/10.3390/microorganisms10061180.
[65] D. Ribitsch, E. Herrero Acero, K. Greimel, A. Dellacher, S. Zitzenbacher, A. Marold, R. Diaz Rodriguez, G. Steinkellner, K. Gruber, H. Schwab, G.M. Guebitz, Polymers 4 (1) (2012) 617–629, https://doi.org/10.3390/polym4010617.
[66] C.V. Aarsen, A. Liguori, R. Mattsson, M.H. Sipponen, M. Hakkarainen, Chem. Rev. 124 (13) (2024) 8473–8515, https://doi.org/10.1021/acs.chemrev.4c00032.
[67] X. Yang, D. Li, C. Song, P. Shao, S. Wang, Z. Wang, Y. Lv, Z. Wei, RSC Adv. 10 (2020) 6414–6422, https://doi.org/10.1039/D0RA00120A.
[68] G. Damonte, B. Barsanti, A. Pellis, G.M. Guebitz, O. Monticelli, Eur. Polym. J. 176 (2022) 111402, https://doi.org/10.1016/j.eurpolymj.2022.111402.
[69] L. Nobs, F. Buchegger, R. Gurny, E. Allémann, Int. J. Pharm. 250 (2) (2003) 327–337, https://doi.org/10.1016/S0378-5173(02)00542-2.
[70] S. Wang, W. Cui, J. Bei, Anal. Bioanal. Chem. 381 (2005) 547–556, https://doi.org/10.1007/s00216-004-2771-2.
[71] A. Pellis, L. Silvestrini, D. Scaini, J.M. Coburn L. Gardossi, D.L. Kaplan, E. Herrero Acero, G.M. Guebitz, Process Biochem. 59 (2017) 77–83, https://doi.org/10.1016/j.procbio.2016.10.014.
[72] V.M. Singh, D. Koo, G.R. Palmese, R.A. Cairncross, J. Appl. Polym. Sci. 120 (5) (2010) 2543–2549, https://doi.org/10.1002/app.33271.
[73] W. Xu, Y. Yang, J. Biomater. Sci. Polym. Ed. 21 (4) (2010) 445–462, https://doi.org/10.1163/156856209x424387.
[74] R. Ghasemi, M. Abdollahi, E.E. Zadeh, K. Khodabakhshi, A. Badeli, H. Bagher, S. Hosseinkhani, Sci. Rep. 8 (2018) 9854, https://doi.org/10.1038/s41598-018-28092-8.
[75] A. Vlachopoulos, G. Karlioti, E. Balla, V. Daniilidis, T. Kalamas, M. Stefanidou, N. D. Bikiaris, E. Christodoulou, I. Koumentakou, E. Karavas, D.N. Bikiaris, Pharmaceutics 14 (2) (2022) 359, https://doi.org/10.3390/pharmaceutics14020359.
[76] S. Adepu, S. Ramakrishna, Molecules 26 (19) (2021) 5905, https://doi.org/10.3390/molecules26195905.
[77] D. Yan, S. Zhang, F. Yu, D. Gong, J. Lin, Q. Yao, Y. Fu, Carbohydr. Polym. 269 (2021) 118341, https://doi.org/10.1016/j.carbpol.2021.118341.
[78] F. Sharif, S. Tabassum, W. Mustafa, A. Asif, F. Zarif, M. Tariq, S.A. Siddiqui, M. A. Gilani, I.U. Rehman, S. MacNeil, Polym. Compos. 40 (4) (2018) 1564–1575, https://doi.org/10.1002/pc.24899.
[79] T. Heunis, O. Bshena, B. Klumperman, L. Dicks, Int. J. Mol. Sci. 12 (4) (2011) 2158–2173, https://doi.org/10.3390/ijms12042158.
[80] T. Mosmann, J. Immunol. Methods 65 (1-2) (1983) 55–63, https://doi.org/10.1016/0022-1759(83)90303-4.
[81] S. Ghorbani, T. Tiraihi, M. Soleimani, J. Biomater. Appl. 32 (6) (2018) 702–715, https://doi.org/10.1177/0885328217741903.
[82] A.M. Pinto, S. Moreira, I.C. Gonçalves, F.M. Gama, A.M. Mendes, F.D. Magalhães, Colloids Surf., B 104 (2013) 229–238, https://doi.org/10.1016/j.colsurfb.2012.12.006.
[83] N. Uzun, T.D. Martins, G.M. Teixeira, N.L. Cunha, R.B. Oliveira, E.J. Nassar, R. A. Dos Santos, Toxicol Lett. 232 (2) (2015) 513–518, https://doi.org/10.1016/j.toxlet.2014.11.032.
[84] K.J. Lampe, R.M. Namba, T.R. Silverman, K.B. Bjugstad, M.J. Mahoney, Biotechnol. Bioeng. 103 (6) (2009) 1214–1223, https://doi.org/10.1002/bit.22352.
[85] K.J. Lampe, K.B. Bjugstad, M.J. Mahoney, Tissue Eng. 16 (6) (2010) 1857–1866, https://doi.org/10.1089/ten.tea.2009.0509.
[86] A.G. Morozov, D.A. Razborov, T.A. Egiazaryan, M.A. Baten'kin, D.Y. Aleynik, M. N. Egorikhina, Y.P. Rubtsova, I.N. Charikova, S.A. Chesnokov, I.L. Fedushkin, J. Polym. Environ. 28 (10) (2020) 2652–2660, https://doi.org/10.1007/s10924-020-01803-x.
[87] J.D. Chea, A. Christon, V. Pierce, J.H. Reilly, M. Russ, M. Savelski, C.S. Slater, K. M. Yenkie, Comput. Aided Chem. Eng. 47 (2019) 199–204, https://doi.org/10.1016/B978-0-12-818597-1.50032-1.
[88] H. Chen, D. Ca, C. Chen, J. Wang, P. Qin, T. Tan, Biotechnol. Biofuels 11 (2018) 286, https://doi.org/10.1186/s13068-018-1284-8.
[89] V. Gerbaud, I. Rodriguez-Donis, L. Hegely, P. Lang, F. Denes, X. You, Chem. Eng. Res. Des. 141 (2019) 229–271, https://doi.org/10.1016/j.cherd.2018.09.020.
[90] N.A. Stini, P.L. Gkizis, C.G. Kokotos, Green Chem. 24 (2022) 6435–6449, https://doi.org/10.1039/D2GC02332F.
[91] L. Cseri, S. Kumar, P. Palchuber, G. Szekely, ACS Sustainable Chem. Eng. 11 (14) (2023) 5696–5725, https://doi.org/10.1021/acssuschemeng.3c00244.
[92] A. Dejaegere, A. Napoli, T.S.A. Heugebaert, C.V. Stevens, Org. Process Res. Dev. 29 (4) (2025) 1076–1082, https://doi.org/10.1021/acs.oprd.4c00494.